

# Perturbation of Charge-Transfer Complexes in Aqueous Solutions of PEG-DNB by Adding *N*-Ethylcarbazole and Li<sup>+</sup> Cations

G. Cojocariu\* and A. Natansohn

Department of Chemistry, Queen's University, Kingston, Ontario K7L 3N6, Canada

Received: December 29, 2002; In Final Form: March 9, 2003

Intramolecular charge-transfer (CT) complexation occurring in aqueous solutions of poly(ethylene glycol) monomethyl ether (PEG) capped at one end with a 3,5-dinitrobenzoyl (DNB) group was perturbed by compounds that interact with either the donor PEG chains or the acceptor DNB group. Hydrophobic *N*-ethylcarbazole (NEK) can be solubilized in aqueous solutions by the PEG-DNB complex surfactant. CT interactions between the NEK solute and the hydrophobic part of the surfactant, the DNB group, favor the solubilization process. The symmetric coplanar sandwich geometry of the NEK/DNB complex does not interfere with the PEG/DNB complex because of the sidewise orientation of the polyether chain. Thus, DNB forms complexes simultaneously with a  $\pi$ -electron donor, NEK, and a p-electron donor, PEG. An interesting consequence of the dual complex is the substantial increase in molecular weight resolution in the NMR spectra. Dissolving LiClO<sub>4</sub> in aqueous solutions of PEG-DNB produces decomplexation. Li<sup>+</sup> cations form ion–dipole interactions with PEG and remove it from its coiled complex with DNB.

## Introduction

Polymer charge-transfer complexes (CT) are extensively investigated for both academic and practical reasons. The presence of intramolecular CT interactions in push–pull azo-containing polymers makes them suitable materials for information optical storage<sup>1–3</sup> and nonlinear optical properties.<sup>4,5</sup> CT interactions are the basis of the electroactive phenomena involved in conductive<sup>6,7</sup> and electroluminescent<sup>8</sup> polymers. Composites of conjugated polymers can be used for photovoltaic cells because of the fast photoinduced CT that can be achieved in these materials.<sup>9</sup> Mesophases can be induced by doping non-liquid-crystalline electron-rich discoid moieties with TNF electron acceptors.<sup>10,11</sup> CT, through the aromatic base stacks of DNA, presents an interesting possibility for using DNA tethered with donor and acceptor groups as a nanowire in future molecular computers.<sup>12–14</sup> CT interactions are also found in high-performance polymers. Polyimides, for example, owe their extraordinary thermal and photochemical resistance, at least in part, to the CT interactions between the *N*-aryl donors and phthalimide acceptors.<sup>15,16</sup>

Recently, we have been investigating the effect of CT complexation on the aggregation of amphiphilic compounds in aqueous solutions. Poly(ethylene glycol) (PEG) end-capped with a 3,5-dinitrobenzoyl group (DNB) shows complex surfactant behavior. The unique combination of amphiphilic character and the ability to form CT complexes is responsible for the properties observed in PEG-DNB aqueous solutions, including unusual <sup>1</sup>H NMR multiplet patterns and molecular weight resolution,<sup>17</sup> complex phase behavior, and new types of composite aggregates.<sup>18</sup> It was previously<sup>18,19</sup> observed that concentration and temperature could be used to alter the conformation of the PEG chain and, consequently, the strength of CT complexation. This resulted in changes in some of the properties of the investigated solution such as color, solubility, or aggregation. In this paper, CT complexation is perturbed by adding a third component that

should be able to replace either the PEG donor or the DNB acceptor in their intramolecular complexes. First, *N*-ethylcarbazole (NEK) is used for its known  $\pi$ -electron donor character<sup>20,21</sup> and therefore its potential to form CT complexes with the DNB acceptor. Model compounds NEK and DNB were used to determine the CT complex geometry by single-crystal X-ray diffraction. Alkali salts are the second type of compound added to aqueous solutions of PEG-DNB. Alkali cations are good electron acceptors, and they are known to form ion–dipole complexes with the oxygen lone pairs of electrons in poly(ethylene glycols).<sup>22–24</sup> The competition between the DNB and the alkali cations in complexing the PEG chains is also investigated here.

## Experimental Section

**Materials.** The synthesis of monomethyl ether poly(ethylene glycol) 3,5-dinitrobenzoate (PEG-DNB) was described previously.<sup>17</sup> *N*-ethyl carbazole (NEK) (Aldrich, 97%) was recrystallized three times from chloroform. 3,5-Dinitrobenzoyl chloride (Aldrich, 98+%) and LiClO<sub>4</sub> (Aldrich, 99.99%) were used as received from freshly open bottles. THF and triethylamine (TEA) were dried before distillation over sodium/benzophenone and CaH<sub>2</sub>, respectively.

**Synthesis of Ethyl 3,5-Dinitrobenzoate (EDNB).** Anhydrous ethanol (25 mL, 0.429 mole) was dissolved together with TEA (2 mL, 0.014 mole) in THF (10 mL). A solution of 3,5-dinitrobenzoyl chloride (3.00 g, 0.013 mole) in 30 mL of THF was added dropwise under stirring while the flask was kept in an ice bath. The solution was allowed to stir for about 4 h under an argon atmosphere at room temperature. The reaction mixture was then filtered to remove the triethylamine chlorohydrate. The white solid obtained after rota-evaporation was purified by recrystallizing twice from ethanol to afford pure EDNB (2.50 g; 80% yield). NMR (CDCl<sub>3</sub>):  $\delta$  1.45 (t, *J* = 7.2 Hz, 3H, –CH<sub>3</sub>), 4.45 (q, *J* = 7.2 Hz, 2H, –CH<sub>2</sub>–), 9.15 (d, *J* = 2.1 Hz, 2H, Ar), 9.2 (t, *J* = 2.1 Hz, 1H, Ar). The melting point determined by DSC is 93 °C (94 °C in ref 25).

\* Corresponding author. E-mail: gheorghe.cojocariu@gepex.ge.com.

**NMR.**  $^1\text{H}$  NMR and 2D NOESY spectra were recorded at  $298.0 \pm 0.1$  K with a variable-temperature 5-mm Bruker BBI probe installed on an AVANCE-400 spectrometer. Deuterated water (Cambridge Isotopes, D 99.9%) was used as a solvent, and 2,2,3,3-*d*(4)-3-(trimethylsilyl)propionic acid sodium salt (Alfa Aesar, 99%) was used as an internal reference (concentration of about 50 ppm). The NEK solubilization was performed in two steps. First, PEG-DNB and NEK were dissolved in chloroform. The solvent was removed by rota-evaporation and then by drying under vacuum for 2 days. The PEG-DNB/NEK mixture was then dissolved in deuterated water. For the alkali cation effect, different amounts of solid  $\text{LiClO}_4$  were added to the PEG-DNB aqueous solutions. The solutions were filtered through Millipore microsyringe filters, having a porosity of  $0.25 \mu\text{m}$ , directly into the NMR tubes. For the NOESY experiments, degassing was done by freeze–thaw cycling under vacuum. After 3 to 5 cycles, there were no more gas bubbles coming out during the thaw. The sealed tubes were stored for at least a week for equilibration before any measurements were made. 2D NOESY experiments<sup>26,27</sup> were performed in the phase-sensitive mode (TPPI),<sup>28</sup> typically using 2K of memory for 512 increments. Mixing times between 0.05 and 1 s were used, and maximum cross peaks were obtained at 0.5 s.

**UV–Visible Spectroscopy.** Electronic spectra were recorded on a Hewlett-Packard 8452A diode array ultraviolet–visible spectrophotometer at room temperature. The samples were prepared in the same way as for NMR (except degassing). Deuterated water was used for aqueous solutions. Chloroform (Aldrich, 99.8% ACS spectrophotometric grade) was used for model compound solutions.

**Thermal Characterization.** DSC thermograms for NEK, EDNB, and the NEK/EDNB complex were recorded on the first heating with a Mettler TC 10 A instrument at a heating rate of  $10^\circ\text{C}/\text{min}$ . DSC thermograms for PEG-DNB and PEG-DNB/ $\text{LiClO}_4$  were recorded on the second heating with a Perkin-Elmer DSC 6 instrument under a nitrogen atmosphere at a heating rate of  $10^\circ\text{C}/\text{min}$ .

**X-ray Crystallographic Analysis.** Complex crystals were obtained from ethanol solutions of NEK/EDNB. Data were collected on a Siemens P4 single-crystal diffractometer with graphite-monochromated  $\text{Mo K}\alpha$  radiation operating at 50 kV and 35 mA at  $23^\circ\text{C}$ . The  $\theta$  range for data collection was between  $2.3$  and  $22.5^\circ$ . Data were processed on a Pentium PC using the Siemens SHELXTL package<sup>29</sup> and were corrected for Lorentz and polarization effects. Neutral-atom scattering measurements were taken from Cromer and Waber.<sup>30</sup> The NEK/EDNB complex crystals belong to the monoclinic system space group  $P2_1/c$  that is uniquely determined by systematic absences. The structure was determined by direct methods. Refinement analysis was performed by full-matrix least-squares analysis on  $F^2$ . All non-hydrogen atoms were refined anisotropically. The positions for all hydrogen atoms were calculated, and their contributions in structural factor calculations were included. The crystallographic data is given in Tables 1 and 2.

**Molecular Orbital Calculations.** The frontier orbitals for NEK and EDNB were calculated with the modeling program HyperChem 3.0, which employs quantum mechanical methods simplified by a semiempirical method, PM3.

## Results and Discussions

**Model Compounds for NEK/DNB  $\pi$ – $\pi$  Interactions.** EDNB was used as a model compound for the DNB group, and its complexes with NEK were investigated both in solution and in the solid state.

**TABLE 1: Crystallographic Data for *N*-Ethylcarbazole/Ethyl 3,5-Dinitrobenzoate**

empirical formula	$\text{C}_{23}\text{H}_{21}\text{N}_3\text{O}_6$	
formula weight	435.43	
wavelength	$0.71073 \text{ \AA}$	
space group	$P2_1/c$	
unit cell dimensions	$a = 19.09(2) \text{ \AA}$	$\alpha = 90^\circ$
	$b = 6.9424(12) \text{ \AA}$	$\beta = 113.11(7)^\circ$
	$c = 17.497(7) \text{ \AA}$	$\gamma = 90^\circ$
volume	$2133(2) \text{ \AA}^3$	
Z	4	
density (calculated)	$1.356 \text{ g/cm}^3$	
absorption coefficient	$1.00 \text{ cm}^{-1}$	
$F_{000}$	912	
crystal size	$0.05 \times 0.5 \times 0.2 \text{ mm}^3$	
$2\theta_{\text{max}}$	$45^\circ$	
limiting indices	$-20 \leq h \leq 18, -7 \leq k \leq 0, 0 \leq l \leq 18$	
reflections collected	2896	
independent reflections	2783 [ $R_{\text{int}} = 0.0394$ ]	
absorption correction	none	
data/restraints/parameters	2782/0/289	
goodness of fit on $F^2$	1.054	
final $R$ [ $I > 2\sigma(I)$ ]	$R_1 = 0.0921, wR_2 = 0.1709$	
$R$ (all data)	$R_1 = 0.2517, wR_2 = 0.2498$	
largest difference peak and hole	$0.210$ and $-0.284 \text{ e \AA}^{-3}$	

**TABLE 2: Selected Bond Lengths ( $\text{\AA}$ ) and Angles (deg) for the EDNB/NEK Complex**

N(1)–C(13)	1.471(9)
C(1)–C(2)	1.372(11)
O(1)–N(2)	1.204(9)
O(2)–N(2)	1.190(8)
O(3)–N(3)	1.224(9)
N(3)–O(4)	1.240(9)
O(5)–C(21)	1.198(10)
O(6)–C(21)	1.300(10)
C(20)–C(21)	1.520(11)
O(2)–N(2)–O(1)	123.0(9)
O(3)–N(3)–O(4)	122.4(10)
C(2)–C(1)–N(1)	128.7(8)
O(6)–C(21)–C(20)	111.1(9)

**Solution Studies.** CT interactions can be identified by the new absorption band that appears at longer wavelengths in the solution of the mixed components, when compared with the spectra of the individual donor and acceptor. Figure 1 shows the electronic spectra of NEK, EDNB, and their 1:1 mixture in chloroform solutions having an overall molar concentration of  $0.05 \text{ mol/L}$ . The absorbance between 400 and 500 nm corresponds to the CT transition band associated with complex formation.

The stoichiometry of the complex is defined as the molar ratio between donor (D) and acceptor (A) molecules and is usually given by simple, integral numbers.<sup>20</sup> However, the coexistence of multiple complexes with various donor/acceptor molar ratios may result in noninteger values for the apparent stoichiometry of the complex.<sup>31</sup> The literature published for complexes of carbazole and DNB derivatives reports different values for the stoichiometry of the complex. Using solid-state NMR, Simmons and Natansohn<sup>32</sup> have observed the formation of an asymmetric 1:1 mole/mole (D/A) complex (Figure 2) between carbazolyl and 3,5-dinitrobenzoyl moieties. There are also studies<sup>33,34</sup> that report the formation of 2:1 mole/mole (D2/A) complexes besides the expected 1:1 mole/mole (D/A) complex. The explanation given for the D2/A complexes<sup>34</sup> resides in the asymmetric structure proposed by Simmons and Natansohn,<sup>32</sup> where the free benzene ring of the carbazole can be engaged in complexation with a second DNB group.

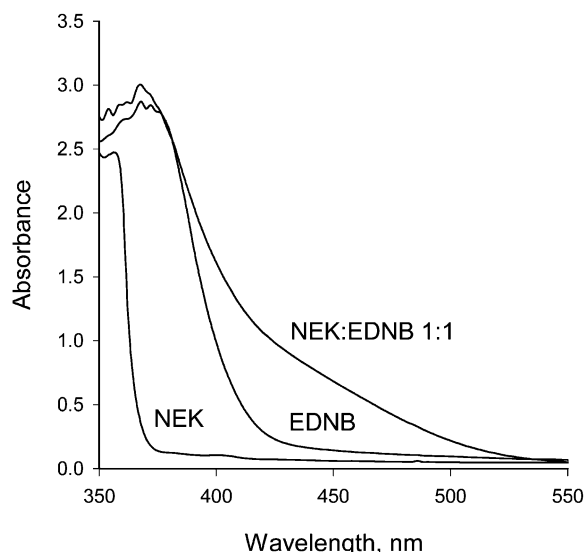


**Figure 1.** UV-vis spectra in 0.05 M chloroform solutions of model compounds.

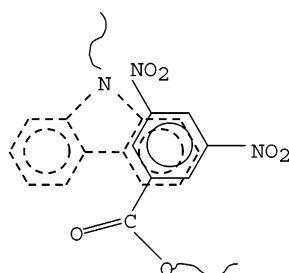


**Figure 2.** Asymmetric complex between carbazoyl and 3,5-dinitrobenzoyl moieties (taken from ref 31).

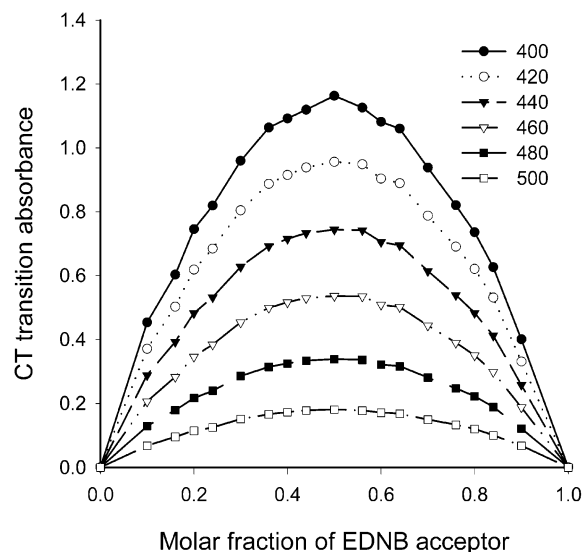


**Figure 3.** UV-vis Job plot for chloroform solutions of NEK/EDNB complexes between 400 and 500 nm.

To investigate the stoichiometry of EDNB/NEK complexes, Job's method<sup>31,35,36</sup> of continuous variation in UV-vis spectroscopy was used. The absorbance is plotted as a function of the molar fraction of donor or acceptor, and the total molar concentration of the solution,  $[D] + [A]$ , is maintained at 0.05 mol/L. The mole fraction ratio at the maximum absorbance point corresponds to the complexation ratio between the two components. Figure 3 shows the Job plot for CT complexation between EDNB and NEK in chloroform solutions. The curve

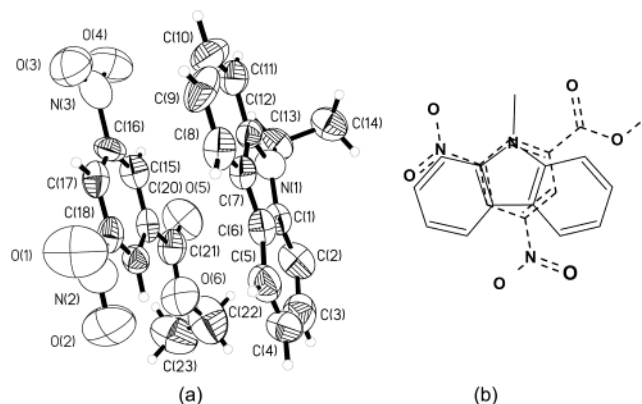


**Figure 4.** Geometry of the NEK/EDNB complex obtained from X-ray crystallography: (a) 50% thermal ellipsoid and labeling diagram and (b) schematics of the complex.

in Figure 3 has a maximum when the donor and the acceptor are in an equimolar ratio, suggesting the formation of a 1:1 mole/mole complex. The symmetry of the curve may also be proof of the presence of only one type of complex.<sup>21</sup> This contradicts the assumptions made previously<sup>33,34</sup> about the bidonor character of the carbazoyl moiety and supports the idea of a single type of equimolecular complex.

**Complex Crystals.** Beside stoichiometry, the geometry of the adduct formed by the donor and acceptor is a very important parameter in characterizing CT complexes. Most of the  $\pi$ - $\pi$  aromatic complexes reported in the literature form a coplanar sandwich structure.<sup>32,37-39</sup> However, there are also reports of other types of configurations. Complexes between anthracene and DNB derivatives were found to form tilted sandwich complexes, where the donor and acceptor rings are tilted at a 20° angle.<sup>40</sup> Edge-to-face configurations were also predicted for intramolecular  $\pi$ - $\pi$  complexes formed in *cis*-1,3-diphenylcyclohexanes.<sup>41</sup> Two reviews have recently documented in detail the intramolecular<sup>42</sup> and intermolecular<sup>43</sup> edge-to-face aromatic interactions.

The X-ray crystallography data obtained on a single crystal of the NEK/EDNB complex is presented in Tables 1 and 2 and Figure 4. The complex crystals are formed of infinite alternating D/A stacks in which NEK and DNB have a coplanar sandwich geometry. The orientation of the DNB ring is centered on the middle ring of the carbazole.

Pearson et al.<sup>21</sup> reviewed the evidence that carbazole and DNB derivatives are able to form both symmetrical and asymmetrical complexes. The geometry determined by X-ray diffraction is symmetrical and is different from the asymmetric complex that was postulated by solid-state NMR.<sup>32</sup> The symmetric complex is in agreement with the 1:1 stoichiometry observed in solution because there is no free carbazole ring to be complexed by a second acceptor molecule.

$\pi$ - $\pi$  complexation between electron donor and acceptor molecules is believed to be favored by CT interactions,<sup>10,11,21,44,45</sup> and the optimum geometry for these interactions is the one that offers maximum overlapping between the HOMO from the donor and the LUMO from the acceptor.<sup>21,44,45</sup> There are also reports that consider that other interactions, such as electrostatic and dispersion forces, are the origin of  $\pi$ - $\pi$  complexation.<sup>40,46-49</sup> The presence of a CT transition band in the visible region of the spectrum suggests that in NEK/EDNB complexes CT interactions play an important role in complex stabilization. To understand the complexation between NEK and EDNB better, we performed molecular orbital calculations at the PM3 level for both molecules to determine the space arrangements of the

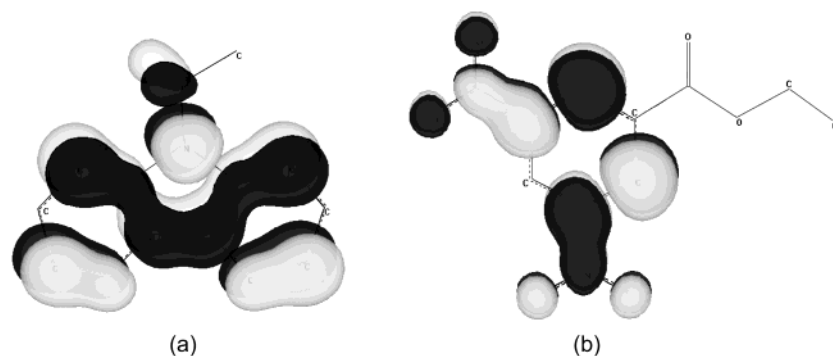


Figure 5. Geometry for (a) the HOMO of NEK and (b) the LUMO of EDNB.

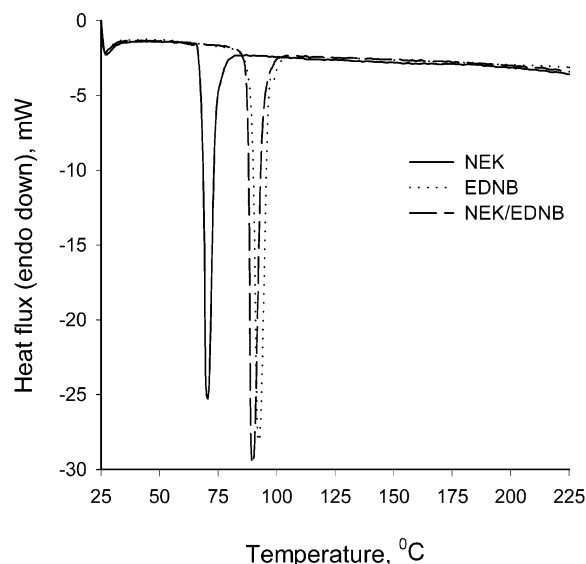


Figure 6. DSC thermograms for NEK, EDNB, and the NEK/EDNB complex. Endothermal signals are pointing down.

HOMO for the NEK donor and the LUMO for the EDNB acceptor (Figure 5). By analyzing the schematics of the complex geometry (Figure 4b) and the location of the HOMO and LUMO orbitals in the donor and acceptor molecules (Figure 5), one can see that the geometry determined by X-ray diffraction corresponds to a maximum HOMO/LUMO overlapping integral. This gives further support for the importance of CT interactions in stabilizing NEK/EDNB complexes.

To determine if there is more than one crystalline form in the solid complexes of NEK/EDNB, DSC thermograms were run for polycrystalline samples. In Figure 6, the thermograms obtained for the complex and the components taken separately are presented. The single narrow and symmetric melting peak obtained for the complex supports the existence of a single type of complex, 1:1 mole/mole as was determined by X-ray diffraction.

**Solubilization of NEK in Aqueous Solutions.** Adding NEK to aqueous solutions of PEG-DNB had a dual purpose. One was to determine how the competing  $\pi$ -electron donor (NEK) will affect the PEG/DNB intramolecular complexes, allowing us to gain more insight into the geometry of these complexes. The other was to test the ability of the complex PEG-DNB surfactant in solubilizing aromatic hydrophobic compounds.

NEK is a solid crystalline aromatic compound that is practically insoluble in water. However, in the presence of the PEG-DNB surfactant, clear homogeneous aqueous solutions containing NEK were obtained. The peaks corresponding to NEK (6.7 to 7.3 ppm) are clearly visible in the proton NMR

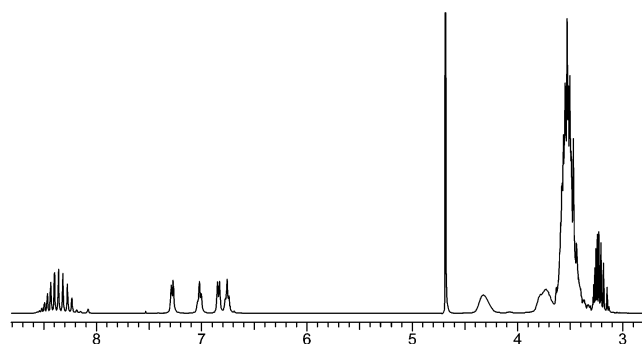


Figure 7.  $^1\text{H}$  NMR of a 15.6 wt % PEG-DNB aqueous solution containing 2.7 wt % solubilized NEK.

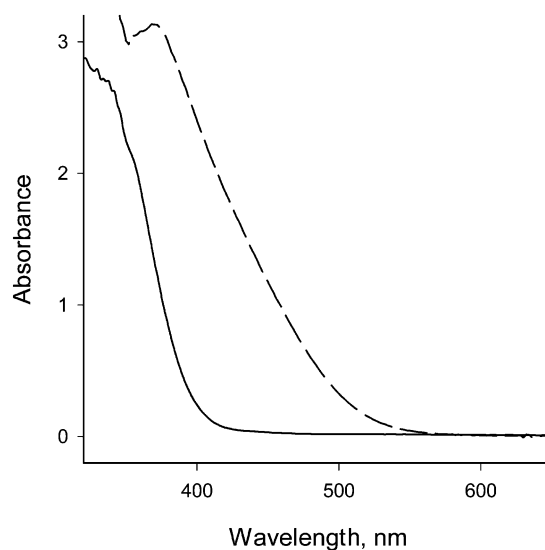
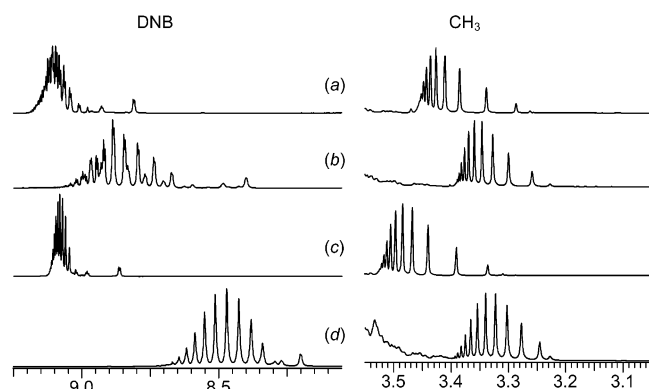


Figure 8. Electronic spectra for a 6.3 wt % PEG-DNB aqueous solution before (—) and after (---) solubilizing 0.5 wt % NEK.

spectrum obtained in a 15.6 wt % PEG-DNB aqueous solution in which 2.7 wt % NEK was solubilized (Figure 7). The absorbance in the visible range of the spectrum drastically increased in solutions containing NEK (Figure 8). This extra absorbance is due to the CT complexes formed between NEK and the DNB group (Figure 1). If NEK is to be solubilized in aqueous solutions of PEG-DNB, then it has to go where the hydrophobic part of the surfactant is located. This means that the solubilization of hydrophobic NEK and its CT complexation with DNB are synergetic.

On the basis of the NMR data, it was demonstrated<sup>18</sup> that the PEG chain is situated sidewise to the DNB ring within the PEG/DNB intramolecular complex. This conformation would also give optimum overlapping between the donor (PEG) and acceptor (DNB) frontier orbitals.<sup>18</sup> Given the different positions



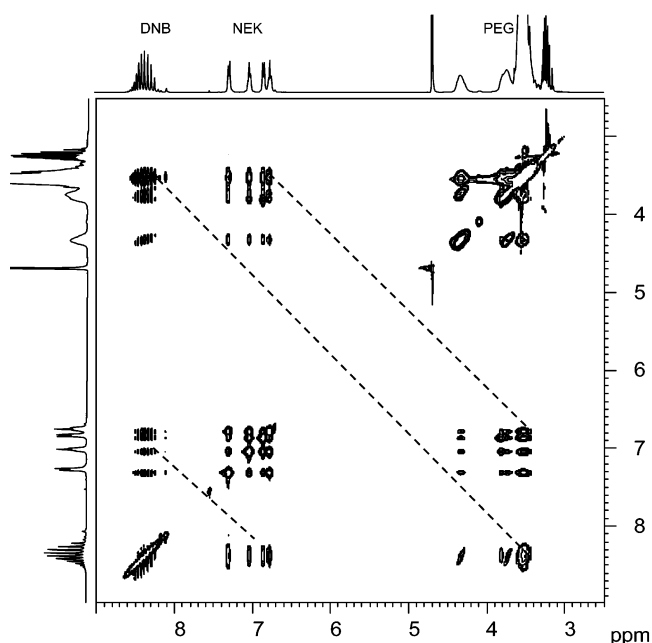


**Figure 9.** Effect of the NEK  $\pi$  donor on the molecular weight resolution of the  $^1\text{H}$  NMR multiplets for two aqueous solutions: (a) 6.3 wt % PEG-DNB with no NEK and (b) with 0.5 wt % NEK and (c) 15.6 wt % PEG-DNB with no NEK and (d) with 2.7 wt % NEK.

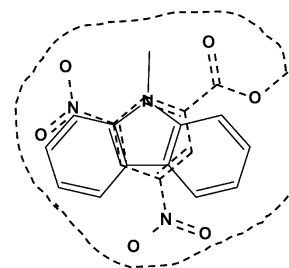
in space occupied by the two different donors, PEG sidewise and NEK coplanar, it should be possible to have them form complexes with DNB simultaneously without too much interference. This possibility is supported by the NMR data obtained in aqueous solutions of PEG-DNB where NEK carbazole was solubilized. The  $^1\text{H}$  NMR spectra of PEG-DNB aqueous solutions at concentrations higher than 4 wt % showed previously<sup>17,18</sup> unusual multiplet patterns for the DNB and methyl peaks. For example, the methyl signal, normally a singlet, was split into 12 peaks. The peaks within the multiplet were assigned to PEG-DNB molecules containing PEG chains of various degrees of polymerization.<sup>17</sup> This molecular weight selectivity of the chemical shift was correlated to the different conformations adopted by CT complexes between DNB and PEG chains of different lengths.<sup>18</sup> One can see from Figure 7 that the multiplet structure of the DNB and methyl peaks is preserved after adding the  $\pi$  donor. This means that the intramolecular CT coil complexes between PEG and DNB are also preserved on adding NEK.

Figure 9 shows a comparison of the multiplet patterns before and after solubilizing NEK in two aqueous solutions having different concentrations of PEG-DNB. It was surprising to see not only that the multiplet patterns did not disappear on adding the second donor but also that their spread (molecular weight resolution) remarkably increased. Both DNB and methyl protons from PEG are substantially shifted upfield (Figure 9), suggesting increased shielding in the solutions containing NEK. This indicates that NEK comes very close to DNB and PEG, allowing the ring currents from NEK to have a strong shielding effect on the chemical shift of both DNB and PEG protons. This observation also supports the coexistence of the two types of complexes,  $p-\pi$  intramolecular PEG/DNB and  $\pi-\pi$  intermolecular NEK/DNB. Further evidence for this premise comes from the 2D NOESY spectra, which shows cross-peak correlation of the DNB group with both NEK and PEG (Figure 10).

The fact that DNB can complex simultaneously with both NEK and PEG is in agreement with the geometry of the intramolecular PEG/DNB complex, where the orientation of the PEG chains is sidewise to the DNB ring.<sup>18</sup> This orientation of the PEG chains leaves the space above and below the DNB ring available for further complexation by NEK. A schematic representation of the  $p-\pi$  and  $\pi-\pi$  complexes' coexistence is given in Figure 11. An important factor in the coexistence of the two complexes is the hydrophobicity of the two  $\pi$ -aromatic systems, NEK and DNB. In the solubilization process, the hydrophobic NEK is directed toward the hydrophobic fragment



**Figure 10.** 2D NOESY NMR spectrum of a 15.6 wt % PEG-DNB aqueous solution containing 2.7 wt % solubilized NEK. Dashed lines indicate the cross peaks between DNB and NEK, DNB and PEG, and NEK and DNB protons.



**Figure 11.** Schematics of the geometry of the NEK/DNB/PEG dual complex. The PEG chain and DNB are drawn with dotted lines.

of the complex surfactant, DNB, and favors the formation of NEK/DNB  $\pi-\pi$  complexes.

The best NMR resolution improvement was observed for the 15.5 wt % PEG-DNB solution containing 2.7 wt % NEK (Figure 9d). These concentrations correspond to a 2:1 molar ratio between PEG-DNB and NEK, which could correspond to a "sandwich" complex with NEK between two PEG-DNB molecules. For the methyl protons, the multiplet shape becomes less skewed after NEK solubilization, resembling more the Gaussian shape of the aromatic multiplet. The symmetry of the methyl multiplet comes from an increase in resolution at the high molecular weight side (downfield), where overlapping was a problem before adding NEK, and a shrinkage at the low molecular weight side (upfield), where peak separation was large anyway. The whole methyl multiplet is shifted upfield (Figure 9c and d) on adding NEK because of the strong ring currents from the carbazole rings. The methyl protons in short PEG complexes are already under the influence of strong ring currents from the DNB group,<sup>18</sup> which probably makes them less sensitive to the carbazole ring currents than the methyl protons in long PEG chains. This may cause the shrinkage observed at the upfield side of the methyl multiplet.

The resolution improvement for the DNB peaks is even more substantial, the multiplet maintaining a Gaussian shape and spreading over about 1 ppm on the chemical-shift scale. The improvement in molecular weight resolution means that the

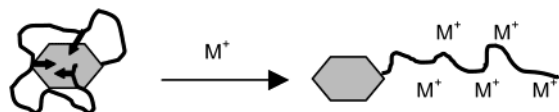


**Figure 12.** Effect of alkali cations ( $M^+$ ) on intramolecular CT complexation.

changes in chemical shift caused by the ring currents and the CT from the added NEK are sensitive to the length of the PEG chain in a manner somehow resembling the intramolecular complexes.<sup>18</sup> In solutions where NEK was solubilized, both UV and NMR indicate that NEK forms a coplanar sandwichlike  $\pi$ - $\pi$  CT complex with the DNB groups. The presence of the PEG chains sidewise to the DNB rings should not prevent the formation of the NEK/DNB complexes, although it may affect the distance between the complexing rings. Therefore, for steric reasons, the shorter the chain, the closer NEK and DNB rings would be and the more shielded the corresponding DNB protons. Under these conditions, although all molecular fractions will experience increased shielding, the increase will be different for molecules of different PEG lengths. This results in further spreading of the DNB multiplet and a resolution improvement by a factor of 3. With this dual complexation, the DNB becomes a "molecular probe" for the local environment of individual oligomers, having a resolution even higher than that of the methyl multiplet. The high resolution can significantly increase the precision for determining MWD by  $^1\text{H}$  NMR<sup>17</sup> and may allow an extension of the method to samples containing slightly longer and more-polydisperse PEG chains.

These results also confirm PEG-DNB to be a good surfactant for aromatic hydrophobic compounds such as carbazolyl derivatives. PEG-DNB has an aromatic moiety as the hydrophobe, as opposed to most of the PEG-based surfactants that contain an alkyl chain as the hydrophobic part. This creates the advantage of easier solubilization of aromatic compounds. Furthermore, the hydrophobic DNB is a good electron acceptor and can form CT complexes with electron donors. The NEK/DNB CT complexation enhances the solubilization affinity between the PEG-DNB surfactant and the NEK solute.

In addition to the two solutions presented here, we also tried to obtain solutions containing a greater amount of NEK. However, samples with PEG-DNB/NEK molar ratios of 1.5:1 and 1:1 could not be dissolved in water. Cloudy liquids, which precipitated eventually, were formed when water was added. The fact that the greatest amount of solubilized NEK corresponds to a 2:1 molar ratio between PEG-DNB and NEK suggests that solubilization requires at least two PEG-DNB surfactant molecules to "sandwich in" every molecule of hydrophobic NEK solute. One can imagine that the NEK molecule will be complexed on each side with a PEG-DNB surfactant molecule in a configuration similar to that shown in Figure 11 (only one side shown for simplicity).

**Effect of Alkali Cations.** Alkali salts were dissolved in aqueous solutions of PEG-DNB to observe the effect of alkali cations on intramolecular complexation. CT complexes between PEG chains and DNB are expected to be destroyed using alkali cations (Figure 12). They have the potential to replace the DNB acceptor because they are known to form ion-dipole complexes with the ether oxygens.<sup>22-24</sup> Figure 13 displays the  $^1\text{H}$  NMR spectra in the aromatic region for a 10.0 wt. % PEG-DNB/ $\text{D}_2\text{O}$  solution containing various amounts of  $\text{LiClO}_4$ . The DNB multiplet is shifted downfield as the amount of added salt is increased. This suggests that CT decomplexation occurs with the polyether oxygens transferring their interacting pairs of electrons to the  $\text{Li}^+$  cations. It can also be seen that adding  $\text{Li}^+$

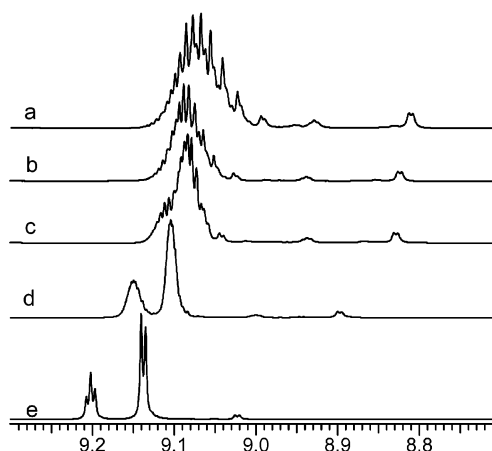


**Figure 13.**  $^1\text{H}$  NMR spectrum in the DNB region for a 15.0 wt % aqueous solution with different EG/ $\text{Li}^+$  molar ratios: (a) no salt, (b) 6.5:1, (c) 2.0:1, (d) 1.0:1.0, (e) 1.0:2.0.

to the PEG-DNB aqueous solution causes the multiplet pattern to disappear gradually, also suggesting CT decomplexation. The complexation between PEG and DNB is affected by the addition of  $\text{LiClO}_4$  in a very similar manner to that previously observed when the solution was diluted or the temperature was lowered.<sup>18</sup> CT complexes are essentially replaced by cation-dipole complexes with a ratio of  $\text{Li}^+/\text{EG}$  of about 2, when "normal" NMR peaks are reestablished. Solid crystalline complexes having EG/ $\text{LiClO}_4$  ratios of 3 and 6 were detected by X-ray diffraction,<sup>50</sup> proving that  $\text{Li}^+$  can have a coordination number of up to 6 EG units. In this case, it takes about two cations per EG unit to remove the intramolecular CT complexation effect on NMR spectra, which is most likely due to salt solvation by water. Strongly solvated  $\text{Li}^+$  will have a considerably lower activity in forming complexes with the PEG chains. The dilution effect and the  $\text{Li}^+$  cation effect on PEG/DNB CT complexation are similar because, analogous to a highly hydrated state, the PEG in  $\text{Li}^+$  adducts is known to have high gauche populations for the  $-\text{C}-\text{C}-$  bonds.<sup>51,52</sup> High gauche populations are unfavorable to the coiled intramolecular CT complexes between PEG and DNB.<sup>18</sup> In addition, the literature<sup>22</sup> mentions that an extended polymer conformation can be caused by a so-called "imposed polyelectrolyte" structure. Lundberg and co-workers<sup>53</sup> observed a dramatic increase in the viscosity of dilute solutions of poly(ethylene oxide) (PEO) as alkali salts were added. They attributed their observations to an "imposed polyelectrolyte" structure caused by the electrostatic repulsion between those sites on the polymer chain where metal cations are coordinated. This effect may also contribute to stretching the PEG chain out of its complex with DNB in the solutions investigated here.

The effect of  $\text{LiClO}_4$  on the CT complexation between PEG and DNB can be seen very clearly in the absence of solvent. Figure 14 shows the DSC thermograms for PEG-DNB and its mixture with  $\text{LiClO}_4$ . The molar ratio between the EG units and the Li salt is 3:1. PEG-DNB alone is an amorphous viscous liquid that does not crystallize even at very low temperatures, as opposed to its poly(ethylene glycol) precursor that is crystalline at temperatures below  $-10^\circ\text{C}$ . The CT interactions require the molecule to adopt a coil conformation, which may be impossible to accommodate into a crystalline lattice.<sup>18</sup> When Li salt is added, the DSC thermogram shows a melting peak at about  $90^\circ\text{C}$ . The literature indicates that, in the solid state,  $\text{LiClO}_4$  can form both crystalline and amorphous complexes with PEG, depending on factors such as salt type and concentration

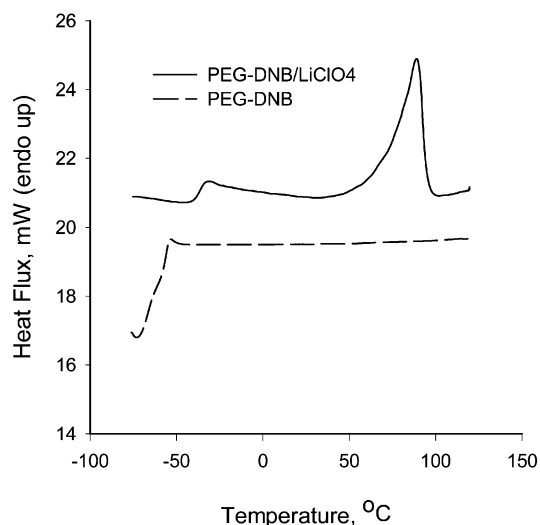


**Figure 14.** DSC thermograms for the PEG-DNB and PEG-DNB/LiClO<sub>4</sub> dry complex. EG/salt = 3:1 mole/mole.

or the solvent used in the preparation step.<sup>22,54</sup> The melting peak observed for PEG-DNB/LiClO<sub>4</sub> is due to the crystalline complexes formed between the Li salt and the PEG chain, which must be in a relatively stretched conformation that allows for packing within a crystal. The PEG-DNB/LiClO<sub>4</sub> mixture is not purely crystalline; an amorphous viscous phase is also formed along with the crystals. This amorphous phase undergoes a glass transition at about  $-36^{\circ}\text{C}$ , which is about  $20^{\circ}$  higher than the glass transition of PEG-DNB alone (Figure 14). This indicates that the amorphous phase is not pure PEG-DNB but is a mixture of PEG-DNB and a Li salt. The ion–dipole interactions between the salt and the amorphous PEG are known to increase the rigidity of the latter, resulting in higher glass transitions.<sup>55–57</sup> The amorphous-phase formation is probably due to inhomogeneities in the salt concentration, with polyether/cation complexes of various stoichiometries coexisting in the system.<sup>54</sup> The polydispersity of the stoichiometry is also the likely reason for the broad melting peak.

## Conclusions

Ethyl 3,5-dinitrobenzoate (EDNB) and *N*-ethylcarbazole (NEK) form a coplanar sandwichlike  $\pi$ – $\pi$  complex with equimolar stoichiometry. Crystallography data obtained from X-ray diffraction on single crystals showed that the complex has symmetric geometry with the DNB ring centered on the middle ring of NEK. This conformation offers a maximum overlapping integral between the frontier orbitals of the donor and acceptor. This fact, together with the strong CT transition band observed in the visible region of the spectrum, indicates that CT interactions make a substantial contribution to complex stabilization.

NEK can be solubilized in aqueous solutions of PEG-DNB that can act as a good surfactant for aromatic hydrophobic compounds. CT complexation between the NEK solute and the hydrophobic part of the surfactant, DNB, favors the solubilization process. The presence of a second electron donor (NEK) in the system does not remove the PEG donor from the intramolecular complex formed with the DNB group. Whereas NEK is situated in parallel planes above or below the acceptor ring, the PEG chains are located sidewise to the DNB ring. Therefore, DNB can simultaneously form complexes with both PEG and NEK. A very interesting consequence of the dual complexes is the drastic increase in the NMR molecular weight

resolution observed with the methyl and aromatic multiplets. The ring currents and the CT effects brought about by the NEK act differently on fractions having PEG chains of different lengths, resulting in significant spreading of the multiplet peaks on the chemical-shift scale.

The effect of adding alkali cations to aqueous solutions of PEG-DNB is very similar to the effect of dilution and reducing the temperature<sup>18</sup> and produces CT decomplexation. The oxygen atoms from PEG can form complexes with alkali cations, donating their lone pair of electrons. The ion–dipole interactions take the PEG chain away from the intramolecular CT complex formed with DNB, causing the DNB NMR multiplet to disappear and be replaced by the “normal” proton spectrum for the DNB protons. In the solid state, the PEG-DNB/Li salt forms both crystalline and amorphous complexes. The crystalline complexes are also proof of the PEG chain being stretched out of its DNB complex by ion–dipole interactions.

**Acknowledgment.** We are grateful to Dr. Suning Wang for X-ray crystallographic analysis and to Dr. Robert P. Lemieux for allowing us to use the HyperChem package for MO calculations. We thank NSERC Canada for financial support. G.C. acknowledges the PGS B Scholarship granted by NSERC.

## References and Notes

- (1) Natansohn, A.; Rochon, P. *Adv. Mater.* **1999**, *11*, 1387.
- (2) Tsutsumi, O.; Kanazawa, A.; Ikeda, T. *Macromol. Symp.* **1997**, *116*, 117.
- (3) Kim, D.-Y.; Lee, T.-S.; Tripathy, S. K.; Jiang, X. L.; Li, L.; Kumar, J. *Macromol. Symp.* **1997**, *116*, 127.
- (4) McBranch, D. W. *Curr. Opin. Solid State Mater. Sci.* **1998**, *3*, 203.
- (5) Dalton, L. R.; Harper, A. W.; Sun, S.; Steier, W. H.; Mustachich, R. V.; Jen, A. K.-Y. *Macromol. Symp.* **1997**, *116*, 135.
- (6) Kang, E. T.; Neoh, K. G.; Tan, K. L. *Prog. Polym. Sci.* **1998**, *23*, 277.
- (7) Garnier, F. *Acc. Chem. Res.* **1999**, *32*, 209.
- (8) Zhang, X. J.; Jenekhe, S. A. *Macromolecules* **2000**, *33*, 2069.
- (9) Brabec, C. J.; Sariciftci, S. N. *Monatsh. Chem.* **2001**, *132*, 421.
- (10) Ringsdorf, H.; Wüstfeld, R.; Zerta, E.; Ebert, M.; Wendorff, J. H. *Angew. Chem., Intl. Ed. Engl.* **1989**, *28*, 914.
- (11) Praefcke, K.; Singer, D.; Kohne, B.; Ebert, M.; Liebmann, A.; Wendorff, J. H. *Liq. Cryst.* **1991**, *10*, 147.
- (12) Holmlin, R. E.; Dandliker, P. J.; Barton, J. K. *Angew. Chem., Intl. Ed. Engl.* **1997**, *36*, 2714.
- (13) Braun, E.; Elchen, Y.; Sivan, U.; Ben-Joseph, G. *Nature* **1998**, *391*, 775.
- (14) Meggers, E.; Michel-Beyerle, M.; Glese, B. *J. Am. Chem. Soc.* **1998**, *120*, 12950.
- (15) Creed, D.; Hoyle, C. E.; Jordan, J. W.; Pandey, C. A.; Nagarajan, R.; Pankasem, S.; Peeler, A. M.; Subramanian, P. *Macromol. Symp.* **1997**, *116*, 1.
- (16) Hasegawa, T.; Horie, K. *Prog. Polym. Sci.* **2001**, *26*, 259.
- (17) Cojocariu, G.; Natansohn, A. *Macromolecules* **2001**, *34*, 3827.
- (18) Cojocariu, G.; Natansohn, A. *J. Phys. Chem. B* **2002**, *106*, 11737.
- (19) Cojocariu, G.; Natansohn, A.; Singh, M. *J. Phys. Chem. B*, submitted for publication, 2002.
- (20) Foster, R. *Organic Charge-Transfer Complexes*; Academic Press: London, 1969.
- (21) Pearson, J. M.; Turner, S. R.; Ledwith, A. In *Molecular Association, Including Molecular Complexes*; Foster, R., Ed.; Academic Press: London, 1979; Vol. 2.
- (22) Wright, P. W. In *Polymer Electrolytes*; MacCallum, J. R., Vincent, C. A., Eds.; Elsevier Applied Science: London, 1989; Vol. 2, Chapter 3.
- (23) von Helden, G.; Wyttenbach, T.; Bowers, M. T. *Science* **1995**, *267*, 1483.
- (24) Besner, S.; Valee, A.; Bouchard, G.; Prud'homme, J. *Macromolecules* **1992**, *25*, 6480.
- (25) Chickos, J. S.; Nichols, G. *J. Chem. Eng. Data* **2001**, *46*, 562.
- (26) Jeneer, J.; Meier, B. H.; Bachmann, P.; Ernst, R. R. *J. Chem. Phys.* **1979**, *71*, 4546.
- (27) Wagner, R.; Berger, S. *J. Magn. Reson., Ser. A* **1996**, *123*, 119.
- (28) Marion, D.; Wuthrich, K. *Biochem. Biophys. Res. Commun.* **1983**, *113*, 967.
- (29) *SHELXTL Crystal Structure Analysis Package*, version 5; Bruker Axs, Analytical X-ray System: Madison, WI, 1995.

- (30) Cromer, D. T.; Waber, J. T. *International Tables for X-ray Crystallography*; Kynoch Press: Birmingham, AL, 1974; Vol. 4.
- (31) Simionescu, C. I.; Grigoras, M. *Prog. Polym. Sci.* **1991**, *16*, 908.
- (32) Simmons, A.; Natansohn, A. *Macromolecules* **1991**, *24*, 3651.
- (33) Setz, S.; Schneider, H. A. *Macromol. Chem. Phys.* **1993**, *194*, 233.
- (34) Bolsinger, M.; Schneider, H. A. *Macromol. Chem. Phys.* **1994**, *195*, 2683.
- (35) Job, P. *Ann. Chim. (Paris)* **1928**, *9*, 113.
- (36) Bassi, I. W.; Bonsignori, O.; Lorentzi, G. P.; Pino, P.; Corradinin, P.; Temussi, P. A. *J. Polym. Sci., Part A-2* **1971**, *9*, 193.
- (37) Hoffman, R. E.; Rabinovitz, M. *Magn. Reson. Chem.* **1993**, *31*, 1031.
- (38) Dahl, T. *Acta Chem. Scand.* **1972**, *26*, 1569.
- (39) Hosomi, H.; Ohba, S.; Ito, Y. *Acta Crystallogr., Sect. C* **2000**, *56*, 147.
- (40) Heaton, J. H.; Bello, P.; Herradon, B.; del Campo, A.; Jimenez-Barbero, J. *J. Am. Chem. Soc.* **1998**, *120*, 12371.
- (41) Williams, V. E.; Lemieux, R. P.; Thatcher, R. J. *J. Am. Chem. Soc.* **1996**, *61*, 1927.
- (42) Jennings, W. B.; Farrell, B. M.; Malone, J. F. *Acc. Chem. Res.* **2001**, *34*, 885.
- (43) Fyfe, M. C. T.; Stoddart, J. F. *Acc. Chem. Res.* **1997**, *30*, 393.
- (44) Sanchez Martinez, E.; Diaz Calleja, R.; Berges, P.; Kudnig, J.; Klar, G. *Synth. Met.* **1989**, *32*, 79.
- (45) Berges, P.; Kudnig, J.; Klar, G.; Sanchez Martinez, E.; Diaz Calleja, R. *Synth. Met.* **1992**, *46*, 207.
- (46) Claessens, C. G.; Stoddart, J. F. *J. Phys. Org. Chem.* **1997**, *10*, 254.
- (47) Blatch, A. E.; Fletcher, I. D.; Luckhurst, G. R. *Liq. Cryst.* **1995**, *18*, 801.
- (48) Bates, M. A.; Luckhurst, G. R. *Liq. Cryst.* **1998**, *24*, 229.
- (49) Cozzi, F.; Cinquini, M.; Annunziata, R.; Siegel, J. S. *J. Am. Chem. Soc.* **1993**, *115*, 5331.
- (50) Robitaille, C. D.; Fauteux, D. J. *Electrochem. Soc.* **1986**, *133*, 315.
- (51) Chatani, Y.; Okamura, S. *Polymer* **1987**, *28*, 1815.
- (52) Takahashi, Y.; Tadokoro, H. *Macromolecules* **1973**, *6*, 672.
- (53) Lundberg, R. F.; Bailey, F. E.; Callard, R. W. *J. Polym. Sci. A-1* **1966**, *4*, 1563.
- (54) Gray, F. M. *Solid Polymer Electrolytes: Fundamentals and Technological Applications*; VCH Publishers: New York, 1991.
- (55) Lauenstein, A.; Tegenfeldt, J. *J. Phys. Chem. B* **1997**, *101*, 3311.
- (56) Smith, M. J.; Silva, C. J.; Silva, M. M. *Solid State Ionics* **1993**, *60*, 73.
- (57) Di Marco, G.; Bartolotta, A.; Carini, G. *J. Appl. Phys.* **1992**, *71*, 5834.